through of the 2.1-kb RNA or initiation in the cellular flanking sequences. The different tissues of E36 1/6 were also analyzed by an immunoperoxidase assay for the presence of HBsAg. A positive but faint staining was seen in all the hepatocytes of E36 1/6 and in a few spleen lymphocytes. This implies an efficient secretion of HBsAg in the serum of the mice. In the liver of a human chronic carrier used as control, about 10 to 20 percent of the cells were detected as strongly positive. Histological examinations of the livers showed a normal liver for E36 1/6 and a mild inflammation for E11.

Finally we analyzed the structure of the serum HBsAg. The density measured in a CsCl gradient was about 1.2 g/ml, which corresponds to that of particles found in infected human serum or in culture medium of HBsAg-producing cell lines. Three mice tested contained in their serum the receptor for polymerized albumin, the product of the pre-S2 region (*18*). The expression of the X gene was not investigated.

Our results show that transgenic mice containing HBV sequences can be used as a model to study the regulation of viral gene expression in vivo. Indeed we have shown that synthesis of the major 2.1-kb S mRNA takes place essentially in the liver of two independent mice producing HBsAg. Although this could be due to integration of pAC_2 in host regions specifically transcribed in liver cells we favor the hypothesis of *cis*-acting control sequences brought in with the injected DNA. This last hypothesis is supported by the recent discovery of a liver specific enhancer element in the HBV genome (*14*). We also show that in the progeny of one animal, males produce more HBsAg than females and that the regulation is at the messenger RNA level in the liver. HBsAg production in hepatoma cell lines has been shown to be inducible by steroid hormones (*19*), but no report has yet mentioned a possible effect of sexual hormones on the virus expression in vivo or in vitro. After 6 months of observation, the animals do not show any signs of pathology. This confirms the current thinking that persistent production of HBsAg, itself, by the chronic carrier is not toxic to the liver. In addition, it is likely that transgenic mice tolerate the presence of the viral antigens since they carry the viral DNA as one of their genes, and thus do not produce antibodies against these antigens. However, it should be possible to induce a liver cell necrosis in these mice and study the influence of the viral sequences on the liver regeneration. The use of other recombinant HBV plasmids will allow a more detailed analysis of the viral gene expression and pathology linked to HBV infection.

References and Notes

1. M. S. Losowski, *Clin. Gastroenterol.* **9**, 3 (1980).
2. R. P. Beasley, *Hepatology* **2**, 21S (1982).
3. H. C. Thomas *et al.*, *ibid.*, p. 116S.
4. C. Bréchot, M. Hadchouel, J. Scotto, M. Fonck, F. Potet, G. N. Vyas, P. Tiollais, *Proc. Natl. Acad. Sci. U.S.A.* **78**, 3906 (1981).
5. J. Summers and W. Mason, *Hepatology* **2**, 61S (1982).
6. J.W. Gordon and F. H. Ruddle, *Science*, **214**, 1244 (1981).
7. R. L. Brinster *et al.*, *Cell* **27**, 223 (1981).
8. P. Grosschedl, D. Weaver, D. Baltimore, F. Costantini, *ibid.* **38**, 647 (1984).
9. R. Palmiter *et al.*, *Nature* (*London*) **300**, 611 (1982).
10. D. Hanahan, *ibid.* **315**, 115 (1985).
11. C. Pourcel *et al.*, *J. Virol.* **42**, 100 (1982).
12. P. Tiollais *et al.*, in *Viral Hepatitis and Liver Disease*, G. N. Vyas, Ed. (Grune and Stratton, Orlando, Fla., 1984), pp. 49-65.
13. R. H. Cattaneo, H. Will, N. Hernandez, H. Schaller, *Nature* (*London*) **305**, 336 (1983).
14. Y. Shaul, W. Rutter, O. Laub, *EMBO J.* **4**, 427 (1985).
15. E. Lacy, S. Roberts, E. P. Evans, M. D. Burtenshaw, F. D. Constantini, *Cell* **34**, 343 (1983).
16. G. H. Swift, R. E. Hammer, R. J. MacDonald, R. L. Brinster, *ibid.* **38**, 639 (1984).
17. D. Morello *et al.*, *Nature* (*London*) **296**, 260 (1982).
18. A. Machida *et al.*, *Gastroenterology* **86**, 910 (1984).
19. N. Huh and T. Otakoji, *Gann* **72**, 178 (1981).
20. J. Meinkoth and G. M. Wahl, *Anal. Biochem.* **138**, 267 (1984).

21. We thank P. Tiollais and E. Wagner for helpful discussion, J. L. Moreau and E. Sobczak for help in performing the radioimmunoassay, and F. Chisari for providing the plasmid pFC80. This work was supported by grants CA37300-02, and CNRS ATP 955225 from the National Institutes of Health and by NATO grant 675 84.

25 June 1985; accepted 10 October 1985

Fractal Surfaces of Proteins

Abstract. *Fractal surfaces can be used to characterize the roughness or irregularity of protein surfaces. The degree of irregularity of a surface may be described by the fractal dimension* D. *For protein surfaces defined with probes in the range of 1.0 to 3.5 angstroms in radius,* D *is approximately 2.4 or intermediate between the value for a completely smooth surface* (D = *2) and that for a completely space-filling surface* (D =*3). Individual regions of proteins show considerable variation in* D. *These variations may be related to structural features such as active sites and subunit interfaces, suggesting that surface texture may be a factor influencing molecular interactions.*

MITCHELL LEWIS
SmithKline and French Laboratories, Philadelphia, Pennsylvania 19101
D. C. REES
Department of Chemistry and Biochemistry, Molecular Biology Institute, University of California, Los Angeles 90024

One of the important problems in structural biology is the origin of specificity and recognition in molecular interactions. An essential step in this process is complementary contact between approaching molecular surfaces. Surface representations of proteins have provided a powerful approach for characterizing the structure, folding, interactions, and properties of proteins (*1*). A fundamental feature of surfaces that has not been characterized by these representations, however, is the texture (roughness) of protein surfaces, and its role in molecular interactions has not been defined. The degree of irregularity of a surface may be described by the fractal dimension D (*2, 3*), where $2 \leq D \leq 3$. As a surface becomes more irregular, the fractal dimension increases from the value $D = 2$, for a smooth surface, to $D \leq 3$.

The value of $(2 - D)$ may be obtained from the slope of the plot of log(surface area) against log(probe size) used to define the molecular surface (*2*):

$$2 - D = \frac{d\log(A_s)}{d\log(R)} \quad (1)$$

where A_s and R are the molecular surface area and probe radius, respectively. Such a relationship is illustrated in Fig. 1 for lysozyme, ribonuclease A, and superoxide dismutase. The slopes of these plots approach zero (corresponding to $D = 2$) in the limit of both small and large probe sizes. Small probes predominantly interact with the smooth van der Waals spheres describing the protein atoms, whereas large probes are sensitive only to the overall shape of the molecule. For probes with radii of 1 to 3.5 angstroms (Å), however, the average value of D is approximately 2.4. Since this size range corresponds to the approximate size of water molecules and side chains, such probes should be sensitive to specific interactions between residues.

To examine the variation in D over protein surfaces, we calculated the fractal dimensions of several proteins and displayed them as spherical projections. The spherical grids were sampled at 10° intervals in the polar angles ϕ and ψ. For each probe size, the surface area was calculated for all atoms within an angle θ about a particular (ϕ, ψ) direction. The

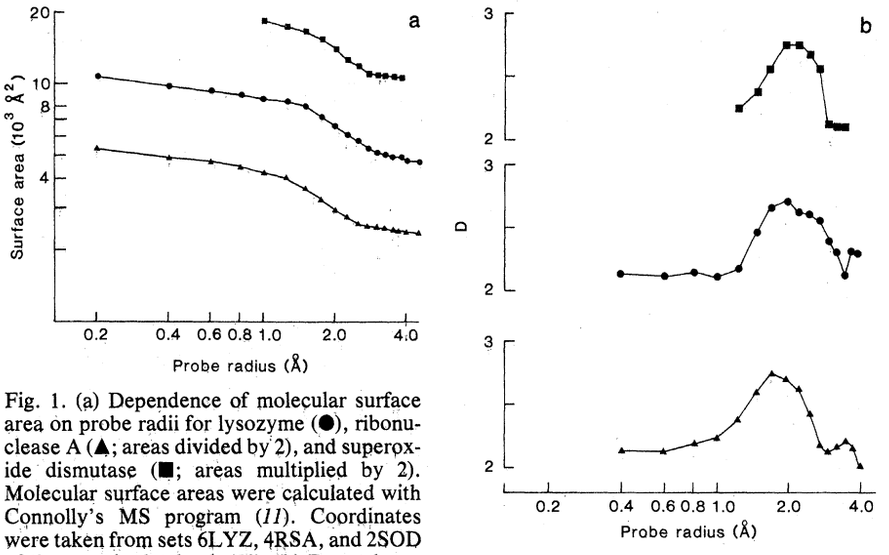

Fig. 1. (a) Dependence of molecular surface area on probe radii for lysozyme (●), ribonuclease A (▲; areas divided by 2), and superoxide dismutase (■; areas multiplied by 2). Molecular surface areas were calculated with Connolly's MS program (*11*). Coordinates were taken from sets 6LYZ, 4RSA, and 2SOD of the protein databank (*12*). (b) Dependence of D on probe radii for the same proteins as in (a). Equation 1 was used to evaluate D as a function of probe radii. The derivative in Eq. 1 was numerically approximated from the data illustrated in (a). Average values of D evaluated for probe radii in the range of 1.0 to 3.5 Å were 2.44, 2.44, and 2.43 for lysozyme, ribonuclease A, and superoxide dismutase, respectively.

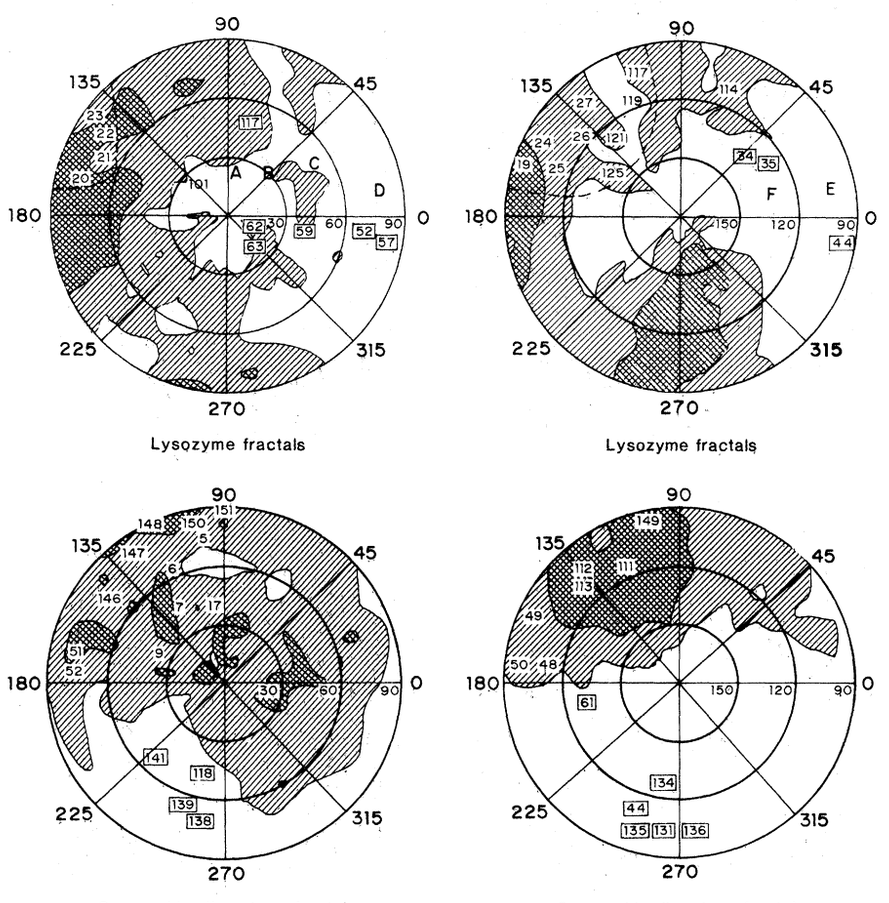

Fig. 2 (top). Spherical projection of the fractal surface of lysozyme. The view is oriented so that the polar angle ψ is measured from the crystallographic z axis. The value of ϕ is measured in the equatorial plane, starting from the crystallographic x axis. Regions with $D > 2.5$ are indicated by crosshatches, and regions with $2.3 \leq D \leq 2.5$ are indicated by diagonal striping. Locations of residues (by number) defining the carbohydrate-binding subsites A to F in the active site (*13*) (residue numbers enclosed within squares) and defining the binding sites for a monoclonal antibody (*4*) are indicated. Fig. 3 (bottom). Spherical projection of the fractal surface for a superoxide dismutase monomer. Regions with $D > 2.5$ are indicated by crosshatches, and regions with $2.3 \leq D \leq 2.5$ are indicated by diagonal striping. Locations of residues (by number) defining the active site (residue numbers enclosed within squares) and the dimer interface are indicated (*14*).

fraction, f, of the spherical surface contained within this cone is given by $0.5(1 - \cos \theta)$. In the present work, $\theta = 30°$ was chosen, with $f = 0.07$. The dependence of D on ϕ and ψ was then established from the variation in the area of each surface element with probe size. The fractal surface of lysozyme calculated in this manner is shown in Fig. 2. The protein surface has patches of high fractal dimension that represent surface irregularities. The surface of lysozyme that cross-reacts with a monoclonal antibody (*4*) consists in part of one of the irregular regions, near residue 22. In contrast, the smoothest surface in lysozyme is associated with residues near the active site. Smoother than average active sites have also been observed for superoxide dismutase (Fig. 3), ribonuclease A, and carboxypeptidase A. The region of greatest surface roughness in superoxide dismutase corresponds to the dimer interface. The same behavior is exhibited by the fractal surface of concanavalin A, in which the most irregular surface region corresponds to subunit interfaces.

Regions of proteins that interact with other proteins to form tight complexes (such as subunit interfaces) appear to be more irregular than average ($D > 2.4$). Regions of proteins that interact transiently with ligands and cannot tolerate formation of stable complexes (such as active sites) appear to be smoother than average. The irregular surfaces apparently form more stabilizing contacts, perhaps by allowing a greater number of van der Waals contacts in a given region than smoother surfaces. A precedent for increased affinity of ligands to rough surfaces comes from studies of metal surfaces. The probability of particles sticking to single crystal surfaces is, in general, higher for atomically rough planes (*5*).

To assess the influence of crystal packing interactions and side-chain motion on fractal surfaces, we calculated a second lysozyme surface for the monoclinic lysozyme structure (protein databank set 1LYM). This crystal form of monoclinic lysozyme is distinct from the tetragonal form used in the fractal calculation of Fig. 2. The two structures were refined independently and have an average coordinate deviation of 1.4 Å (0.6 Å for the main-chain atoms and 1.9 Å for the side-chain atoms). The fractal surface for the monoclinic structure was not significantly different from that for the tetragonal structure. This indicates that crystal packing and small differences in side-chain conformations have no major effect on the fractal surfaces. The relative insensitivity of fractal surfaces to the

precise location of individual atoms (within 1 to 2 Å) is in part due to the cone-averaging procedure utilized in the fractal surface calculation. A second factor is that surface area calculations also appear to be insensitive to the fine details of residue structure and conformation, as indicated by the successful application of several simplified and statistical approaches for the calculation of surface area (*6, 7*).

We also examined whether D may be related to such properties as residue mobility or exposed surface area to establish whether fractal surfaces provide an independent characterization of surface properties. Comparisons of D to the refined temperature factors for myoglobin (protein databank set 1MBD) and superoxide dismutase indicate that these parameters are unrelated. As measured with small probes ($R < 2$ Å), the value of D also appears to be unrelated to exposed surface area. Regions of proteins accessible to larger probes, however, tend to be associated with smooth regions of the fractal surface. Intuitively, this relation appears to be reasonable since residues on smooth surfaces are more likely to be able to contact large probes than residues on irregular surfaces. These considerations suggest that the calculation of fractal surfaces, like the calculation of residue mobility (*8, 9*), may be a useful technique for describing the antigenic determinants on a protein.

Fractal surfaces provide a means for characterizing the irregularity of protein surfaces. These surfaces are irregular when viewed on an atomic scale, with an average fractal dimension of about 2.4. A high degree of irregularity in proteins is consistent with direct experimental measurements of the fractal dimension of the polypeptide backbone (*10*). Rather than being uniformly irregular, however, the degree of irregularity varies across the protein surface. Regions involved in the formation of tight complexes (such as interfaces and possibly antibody-combining regions) appear to be more irregular than regions involved in the formation of transient complexes (such as active sites). Recognition of these geometric factors provides a new approach to describing the interaction of macromolecules with one another.

References and Notes

1. F. M. Richards, *Annu. Rev. Biophys. Bioeng.* **6**, 151 (1977).
2. B. B. Mandelbrot, *The Fractal Geometry of Nature* (Freeman, San Francisco, 1983).
3. D. Avnir, D. Farin, P. Pfeifer, *Nature (London)* **308**, 261 (1984).
4. A. Amit *et al.*, *ibid.* **313**, 156 (1985).
5. G. Somorjai, *Chemistry in Two Dimensions: Surfaces* (Cornell Univ. Press, Ithaca, N.Y., 1981).
6. M. Levitt, *J. Mol. Biol.* **104**, 59 (1976).
7. S. J. Wodak and J. Janin, *Proc. Natl. Acad. Sci. U.S.A.* **77**, 1736 (1980).
8. E. Westhof *et al.*, *Nature (London)* **311**, 123 (1984).
9. J. A. Tainer *et al.*, *ibid.* **312**, 127 (1984).
10. J. P. Allen, J. T. Colvin, D. G. Stinson, C. P. Flynn, H. J. Stapleton, *Biophys. J.* **38**, 299 (1982).
11. M. Connolly, *J. Appl. Crystallogr.* **16**, 548 (1983).
12. F. Bernstein *et al.*, *J. Mol. Biol.* **112**, 535 (1977).
13. L. O. Ford, L. N. Johnson, P. A. Machin, D. C. Phillips, R. Tjian, *ibid.* **88**, 349 (1974).
14. J. A. Tainer, E. D. Getzoff, K. M. Beem, J. S. Richardson, *ibid.* **160**, 181 (1982).

15. Supported in part by NIH grant GM31875, Chicago Community Trust/Searle Scholars Program, and an NSF young investigators award (D.C.R.).

17 May 1985; accepted 23 September 1985

Synthesis and Evaluation of a Prototypal Artificial Red Cell

Abstract. *A new process allows microencapsulation of purified human hemoglobin and 2,3-diphosphoglycerate to form neohemocytes. The microcapsule membrane is composed of phospholipids and cholesterol. Neohemocytes are substantially smaller than erythrocytes, contain 15.1 grams per decaliter of hemoglobin, and have a* P_{50} *value (the partial pressure of oxygen at which the hemoglobin is half-saturated) of 24.0 torr. All rats given 50-percent exchange transfusions survived with only limited evidence of reversible toxicity. Normal serum glutamate-pyruvate-transaminase values at 1, 7, and 30 days after transfusion were consistent with minimal hepatotoxicity. The concentration of blood urea-nitrogen was elevated by 35 percent after 1 day but returned to normal by day 7. However, histopathology revealed normal kidneys on day 1 as well as on days 7 and 30. Neohemocytes cleared from the circulation of transfused rats with an apparent half-life of 5.8 hours.*

C. ANTHONY HUNT
RONALD R. BURNETTE*
RODERICK D. MACGREGOR
ANNE E. STRUBBE
School of Pharmacy, University of California, San Francisco 94143
DANIEL T. LAU
Animal Care Facility, University of California, San Francisco 94143
NOEL TAYLOR
Electron Microscopy Laboratory, Veterans Administration Medical Center, San Francisco, California 94121
HIROSHI KAWADA
Faculty of Pharmaceutical Sciences, Science University, Tokyo 162, Japan

*Current address: Department of Pharmaceutical Chemistry, University of Wisconsin, Madison 53706.

We now report the synthesis of artificial red cell prototypes that meet the six essential specifications for such cells: (i) the microcapsule membrane must be biodegradable and physiologically compatible; (ii) the encapsulation process must avoid significant hemoglobin (Hb) degradation; (iii) when encapsulated, the oxygen affinity of Hb must be reduced relative to that of free human Hb; (iv) the encapsulated Hb must be sufficiently concentrated, that is, more than 33 percent of that in erythrocytes; (v) there should be no evidence of overt intravascular coagulopathy; and (vi) the artificial cells must be small enough to pass unrestricted through normal capillaries. We call these prototypal artificial red cells neohemocytes (NHC).

Microcapsules with lipid bilayer membranes rather than biodegradable polymer (*1*) or polymerized protein membranes (*2*) were used to make the artificial cells, and the procedure (*3*) was based on one used for the preparation of liposomes (*4*). The preparation of each batch started with 0.293 mmol of human hemoglobin and 3.75 mmol of lipid consisting of egg yolk phosphatidylcholine, dipalmitoylphosphatidic acid, cholesterol, and α-tocopherol in a molar ratio of 4:1:5:0.1, respectively. The resulting NHC were relatively homogeneous in size but less than homogeneous in content (Fig. 1). The pellet from a 25 percent suspension of NHC contained an average (n = 10 batches) of 151 mg/ml [(standard deviation (SD), 4)] of Hb and 2.21 mg/ml (SD, 0.11) of total lipid. The mean concentration of Hb within NHC was 15.8 g/dl. Only about 4.4 percent of the total displaced volume of NHC was membrane, if a lipid density of 1 g/cm^3 is assumed. Additional characteristics of the cells are listed in Table 1.

The pharmacokinetic properties of NHC were analyzed by following coencapsulated tracer amounts of ^{14}C-labeled sucrose in five rats that had undergone a 50 percent exchange transfusion (*5*). The amount of ^{14}C found in the blood of these rats thus reflected the amount of circulating, encapsulated sucrose and was taken as a direct measure of those NHC remaining intact in circulation (*6*). After 8 hours the mean amount of ^{14}C in the blood dropped to 40 percent of its value immediately after transfusion, with an